

Morphological Changes in Segmented Polyurethane Elastomers by Varying the NCO/OH Ratio

G. SPATHIS,^{1,*} M. NIAOUNAKIS,¹ E. KONTOU,¹ L. APEKIS,² P. PISSIS,² and C. CHRISTODOULIDES²

¹Department of Theoretical and Applied Mechanics, and ²Department of Physics, National Technical University of Athens, 5 Heroes of Polytechniou Ave., 157 73 Athens, Greece

SYNOPSIS

The morphological changes induced to segmented polyurethane elastomers by varying the NCO/OH ratio during the second step of polymerization, while keeping constant the total hard-segment content ($\sim 30\%$), were studied by means of Fourier transform infrared spectroscopy (FTIR), differential scanning calorimetry (DSC), and the thermally stimulated depolarization current method (TSDC). The DSC results gave evidence for the existence of phase separation in thermoplastic polyurethanes, whereas the elastomeric ones appeared to form a more homogeneous network. The FTIR results gave additional evidence regarding phase separation by detecting the strength of the hydrogen bonds. Moreover, an attempt was made to assess the relative contribution made to the hydrogen bonding in such systems by the two potential acceptors: ester and urethane carbonyls. The TSDC results gave a relaxation mechanism that is due to interfacial (Maxwell-Wagner-Sillars) polarization, providing evidence of the existence of an interfacial phase. The introduced secondary chemical cross-links was found to affect mainly the irregularly packed hard domains and to form a more homogeneous network at higher values of the NCO/OH ratio.

© 1994 John Wiley & Sons, Inc.

INTRODUCTION

The domain structure that results from phase segregation of the hard and soft segments in polyurethane-segmented copolymers is well recognized as the principal feature controlling the properties of this class of elastomers.¹ Considerable effort has been made in understanding the character of the domain structure and some literature reviews²⁻⁵ are available. From these reviews, it is recognized that a wide variety of variables, such as the types of hard and soft segments, molecular weight, and molecular weight distribution of the two components, the chain extender, the stoichiometric ratio between them, the processing history, and the polymerization method, will affect the degree of phase separation and hard-segment domain size and, accordingly, the bulk and surface properties of the polymers.

Relatively few data have been published concerning the effect of the NCO/OH ratio on the properties of linear segmented polyurethane elastomers. Redman⁴ reported the effect of the NCO/OH ratio on molecular weight and on the rheological, thermal, and mechanical properties of two series of ester-based polyurethanes. Nierzwicki and Wysocka⁶ also studied the effect of the NCO/OH ratio on the microphase separation of ester-based polyurethanes. For NCO/OH > 1, because of the excess diisocyanate, allophanate cross-links are formed. The introduction of chemical cross-links has a detrimental effect on the hard domains, namely, the physical cross-links of the copolymer. In a previous article,⁷ it was shown that increased chemical cross-linking leads to reduction in the size and the number of hard domains, changes the morphology, and causes mixing of hard and soft segments.

Two of the most widely used techniques to detect and measure the different types of domain structure present in a segmented polyurethane elastomer are Fourier transform infrared spectroscopy (FTIR) and differential scanning calorimetry (DSC). Infrared

* To whom correspondence should be addressed.

spectroscopy has been used as the principal technique to characterize the different hydrogen bonds formed and to infer phase-separated structures in polyurethanes.^{8,9} DSC provided additional information about the morphology via analysis of the melting behavior and by measuring the heat capacity change of the soft segment at the glass transition temperature.^{10,11}

In the present work, the changes to the phase-separation structure caused by varying the NCO/OH ratio were studied by DSC and FTIR in conjunction with the thermally stimulated depolarization current method (TSDC). A major feature of the TSDC is that it offers the possibility to experimentally resolve relaxation processes arising from sets of dipoles with slightly different relaxation times. The analysis of a relaxation mechanism makes it possible to obtain the activation energy W , the preexponential factor τ_0 , and the contribution of the mechanism to the static permittivity $\Delta\epsilon$.¹² The method of TSDC is, also, an experimental tool that is sensitive to relaxation processes inside the interfacial layers and provides new possibilities for the study of such morphological details in polyurethanes.

A series of poly(ester-urethane) block copolymers were prepared via a two-step polymerization process while the hard-segment content was maintained at about 30% and the molecular weight altered by preparing the polymers at five different NCO/OH ratios. The effects of the NCO/OH ratio on the stability of the hard phase and on the relaxation of the soft part were investigated.

MATERIALS

The synthesis was carried out by a two-step polymerization process involving end capping the hydroxy-terminated polyester (PEA) with the diisocyanate (MDI) followed by reaction with the chain extender (BDO). The details of the procedure have been described previously.⁷ The polyester used was poly(ethylene adipate) (Desmophen 2000, Bayern AG) with an average molecular weight of 2000. The diisocyanate was diphenylmethane diisocyanate (Desmodur 44, Bayern AG) and the chain extender was 1,4-butanediol.

The NCO/OH ratio during the second step of polymerization was taken at the values 0.9, 1.0, 1.1, 1.2, and 1.3 at a fixed prepolymer composition with a molar ratio of MDI/PEA equal 2.8/1.0. The five

samples were designated by the NCO/OH ratio value (i.e., EPU10).

EXPERIMENTAL

Infrared Spectroscopy

Thin films for the infrared studies were prepared either by solution casting or from the melt. For the solution-cast films, 5% (w/v) of the polymer was dissolved in THF and poured onto KBr glass plates. The four samples were then placed in a vacuum oven and annealed at 110°C for 24 h.

Infrared spectra were obtained with a computerized Bruker IFS 113V Fourier transform infrared spectrometer. All the measurements were carried out in a vacuum at room temperature. For each sample, 32 scans at 2 cm⁻¹ resolution were collected in the absorption mode and stored in the memory of the computer. The spectra were then analyzed employing a curve-resolving technique based on a linear least-squares analysis to fit a combination of the Lorentzian and Gaussian curve shapes.

Integrated absorbances were corrected for sample thickness differences using the C=C stretching vibration in the aromatic ring at 1595 cm⁻¹ as a normalizing factor. By analyzing the characteristic infrared bands of the isocyanate group at 2265 cm⁻¹, no residual isocyanate groups were detected in any of the materials tested.

The frequency shift is defined as

$$\Delta\nu = \nu_f - \nu_b \quad (1)$$

where ν_f and ν_b are the frequencies of maximum absorption for the free and hydrogen-bonded N—H groups, respectively. The shift, $\Delta\nu$, in the stretching frequency of the hydrogen-bonded N—H group, is considered a measure of the strength of the hydrogen bond. As the hydrogen bond strengthens, the (N—H···O—C) distance, measured in the solid state by X-crystallography, decreases and this decrease is usually accompanied by an increase in the difference between the associated N—H stretching frequency and the nonassociated N—H stretching frequency.¹³

Differential Scanning Calorimetry (DSC)

The DSC measurements were made using a DuPont 9000 thermal analyzer with the DSC module at a programmed heating rate of 20°C. The cell was calibrated using indium and tin standards. The sample size was 10–15 mg.

Thermally Stimulated Depolarization Current (TSDC)

The TSDC method is as follows¹²: The sample is polarized by an applied electric field E_p at a temperature T_p . This polarization is subsequently frozen in by cooling the sample to a temperature T_0 sufficiently low to prevent depolarization by thermal energy. The field is then switched off and the sample is warmed at a constant rate b , while the depolarization current, as the dipoles relax, is detected by an electrometer. Thus, for each polarization mechanism, an inherent current peak can be detected. In the case of a single relaxation process obeying the Arrhenius equation, $\tau(T) = \tau_0 \exp(W/kT)$, the depolarization current density $J(T)$ is given by the equation

$$J(T) = \frac{P_0}{\tau_0} \exp(-W/kT) \times \exp\left[-\frac{1}{b\tau_0} \int_{T_0}^T \exp(-W/kT') dT'\right] \quad (2)$$

where τ is the relaxation time; W , the activation energy of the relaxation; τ_0 , the preexponential factor; T , the absolute temperature; k , the Boltzmann's constant; and P_0 , the initial polarization.

The samples measured were cylindrical discs of about 13 mm diameter and various thicknesses (0.51–2.17 mm). Typical values for the experimental conditions were 27°C for the polarization temperature, 5 min for the polarization time, 10°C/min for the cooling rate down to -196°C, 3°C/min for the heating rate, and 3.5–13 kV/cm for the polarizing electric field.

RESULTS

The composition of the investigated polyurethanes is given in Table I. As can be seen, all the samples

have the same hard-segment content ($\sim 30\%$), while the NCO/OH ratio, during the second step of polymerization, was varied. Therefore, the hard-segment distribution, the domain morphology, and their contribution to the elastic behavior are different for all the materials prepared.

FTIR Results

The infrared spectrum of a representative polyurethane sample, recorded at room temperature, is shown in Figure 1. Several spectral regions are involved in the hydrogen bonding, i.e., N—H stretching, C=O stretching (amide I), N—H in-plane bending (amide II), and out-of-plane deformation (amide V).¹³ The first two regions are the subject of the present investigation. The N—H stretching is in the 3500–3200 cm^{-1} region and the C=O stretching is in the 1760–1620 cm^{-1} region. In Figure 2 are presented the FTIR spectra in the N—H stretching region of the four polyurethane samples. The strong band is assigned to the hydrogen-bonded N—H stretching vibration, and the weak shoulder on the high-frequency side of this band, to the free N—H stretch. The hydrogen-bonded N—H band sharpens and shifts to higher frequencies as the NCO/OH ratio varies from 0.9 to 1.2. The frequency shift can be explained as a decrease in the average strength of the hydrogen bonds.

Curve fitting of the N—H stretching region was performed on every spectrum. Figure 3 shows the results of the curve-fitting procedure for two representative samples. The N—H stretching region of each sample is analyzed into four components: Two of them correspond to "free" and hydrogen-bonded N—H groups. The other two bands are attributed to two phonon vibrations.¹⁴ The curve-fitting analysis for the N—H stretching region of each polyurethane sample is given in Table II.

The "free" N—H stretching band occurs at approximately 3451 cm^{-1} . The area of this band in-

Table I Molar Compositions of the Five Investigated Samples

Materials' Designation	Molar Ratio MDI : PEA : BDO	Hard-segment Content wt % (MDI + BDO)*
EPU09	2.8:1:2.00	30.5
EPU10	2.8:1:1.77	30.0
EPU11	2.8:1:1.64	30.0
EPU12	2.8:1:1.50	29.5
EPU13	2.8:1:1.38	29.2

* Calculated as weight percentage of MDI and BDO per total polymer weight.

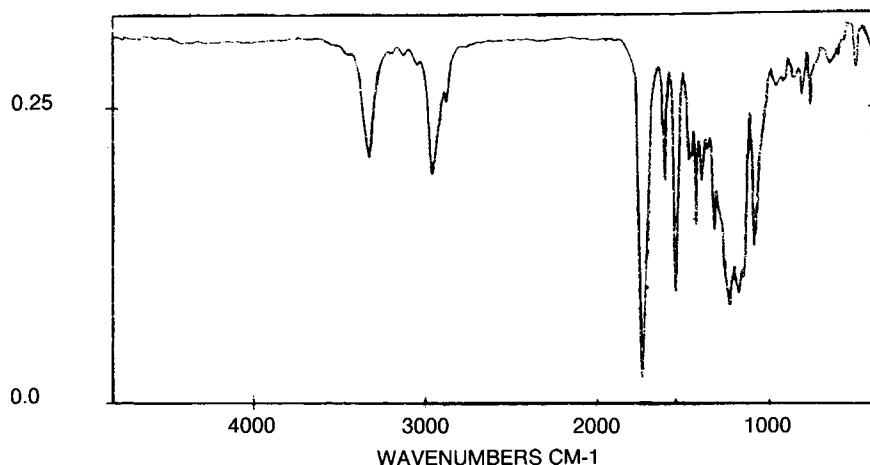


Figure 1 Infrared spectrum of EPU09 sample recorded at room temperature.

creases by a factor of 8 as we move from the thermoplastic to elastomeric polyurethanes. However, taking into account the difficulties in accurately measuring this band, plus the fact that the absorptivity coefficient is expected to vary with the NCO/OH ratio, led us to conclude that these results are nothing else but qualitative.

As can be seen in Figure 2, the materials are divided in two groups: The first group, which includes the samples EPU09 and EPU10 (thermoplastic), has broad and asymmetrical N—H bands that encompass, at least, three components each. The second group, which includes the samples EPU11 and EPU12 (elastomeric), has sharp and symmetrical bands with two components each. The frequency

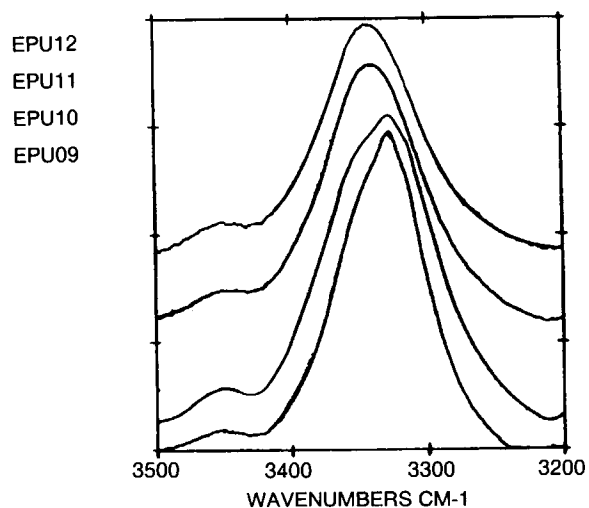


Figure 2 FTIR spectra in the N—H stretching region of the four investigated samples.

shift of the hydrogen-bonded N—H stretch is for the first group 123 cm^{-1} , and for the second, 109 cm^{-1} (see Table II).

In Figure 4 are presented the FTIR spectra in the C=O region of the four polyurethane samples. The subgroup of the thermoplastic polyurethane samples exhibit a weak shoulder at 1700 cm^{-1} that is assigned to hydrogen-bonded urethane carbonyls.

The C=O stretching region of each sample is analyzed into three components. Curve fitting of the C=O stretching region was performed on every spectrum. Figure 5 shows the results of the curve-fitting procedure for two representative samples. These are attributed to “free” and hydrogen-bonded (ordered plus disordered) C=O groups. The curve-fitting analysis for the C=O stretching region of each polyurethane sample is given in Table III.

TSDC Results

In Figure 6, the TSDC plots of two representative samples are shown. The plots show a broad dispersion with two maxima, at about 110 and 160 K in the low-temperature region, and two peaks, one between 235 and 245 K (peak I) and another appearing between 255 and 270 K (peak II), in the high-temperature region. Measurements show that the low-temperature peaks have practically the same shape and magnitude for all the types of polyurethanes studied, while their position shifts to higher temperatures as the NCO/OH ratio increases.

Figures 7 and 8 show for peaks I and II, respectively, their position in the TSDC plots (peak temperature T_M) and their magnitudes (current maxima I_M normalized to the same polarizing field, heating

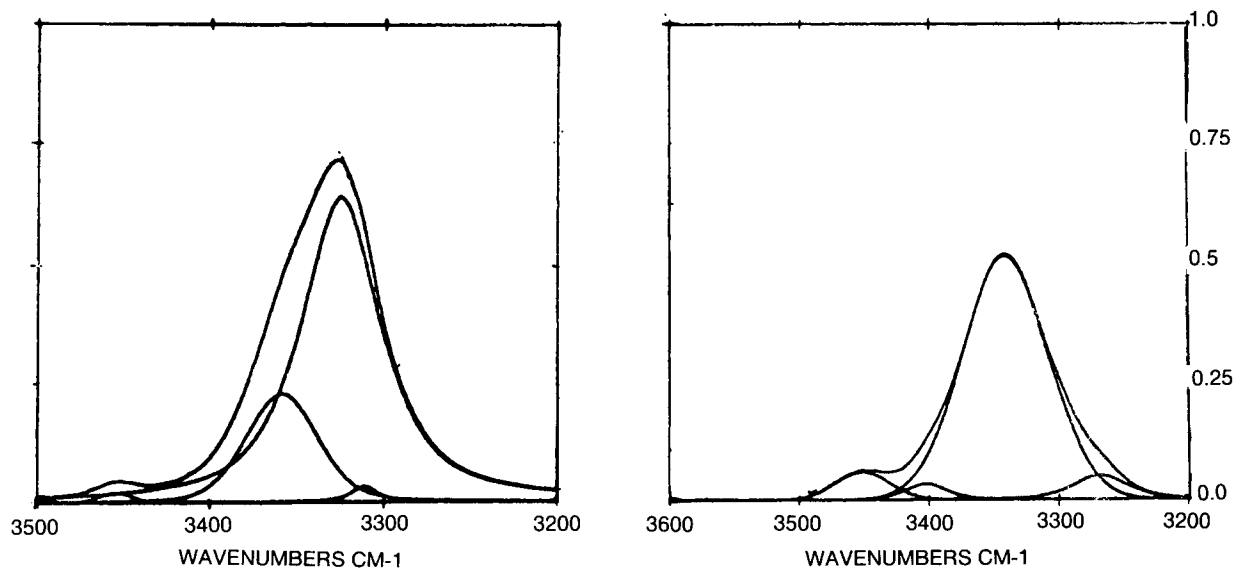


Figure 3 Curve-fitting analysis in the N—H stretching region of two representative samples with NCO/OH ratio values 0.9 and 1.2, respectively.

rate, and cross section for all samples) for the five types of polyurethane studied. The results are plotted as a function of the NCO/OH ratio. As can be seen, the maximum temperature of peak I shifts to higher values and its magnitude increases slightly as the NCO/OH ratio increases. On the contrary, the peak temperature of peak II shifts to lower values and its magnitude decreases as the NCO/OH ratio increases.

Peak I has been analyzed into simpler components by the thermal sampling (TS) technique.¹² The TS technique consists of "sampling" a relaxation process within a narrow temperature range by means of polarization at a certain temperature, followed by depolarization at a temperature a few degrees lower, in order to isolate some of the relaxation components. A typical spectrum of activation energies of peak I obtained by TS analysis is presented in Figure 9. The activation energy, W , and the

preexponential factor, τ_0 , of the main component of peak I, obtained by TS analysis, vs. the NCO/OH ratio are presented in Figure 10.

DSC Results

The DSC thermograms of the five tested polyurethanes, in the temperature range from -100 to 100°C , are shown in Figure 11. As can be seen, the glass transition temperature is shifted to higher temperatures as the NCO/OH ratio is increased. The glass transition temperature values, T_g and the heat-capacity changes, ΔC_p , accompanying this transition are listed in Table IV.

Above ambient temperatures, samples with NCO/OH < 1 exhibit a sharp endothermic peak at about 50°C , whereas samples with NCO/OH > 1 do not have an analogous behavior. Moreover, the

Table II Curve-fitting Analysis Results of the N—H Stretching Region for Each Polyurethane Sample

Sample	"Free" N—H			Hydrogen-bonded N—H			$\Delta\nu_s$ (cm^{-1})
	ν_f (cm^{-1})	Integral	Width	ν_b cm^{-1}	Integral	Width	
0.9	3454	0.15	22.3	3325	15.50	56.	129
1.0	3452	0.12	20.2	3322	15.80	57.3	130
1.1	3449	1.28	46.	3341	14.76	78.9	109
1.2	3452	0.93	49.6	3341	12.81	77.5	110

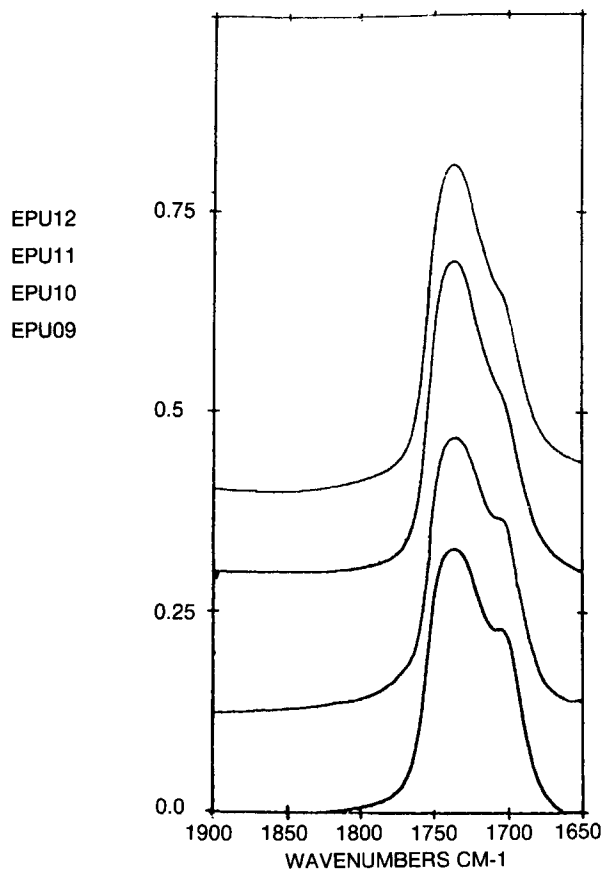


Figure 4 FTIR spectra in the C=O stretching region of the four investigated samples.

intensity of this peak was shown to increase with time at room temperature.

In addition, samples with NCO/OH < 1 exhibit a small broad endotherm at about 80°C. The area of this peak diminishes in sample EPU11 and vanishes for EPU12. At higher temperatures (see Fig. 12), the samples EPU09 and EPU10 exhibit two distinct endothermal peaks, while the thermogram of EPU11 has only one broad main endotherm. Finally, the thermogram of EPU12 exhibits only one main, sharp, endotherm at a lower temperature.

DISCUSSION

Boyartchuk et al.,¹⁵ on the basis of solution studies, obtained N—H frequency shifts of 80–90 cm^{-1} for hydrogen bonding with an ester C=O and 130 cm^{-1} for hydrogen bonding with a urethane C=O. Our data, on the thermoplastic subgroup of polyester urethanes, showed a $\Delta\nu_s = 129 \text{ cm}^{-1}$, indicating, from the above frequency shifts, a preponderance of hydrogen bonding with urethane C=O groups. The data on the elastomeric subgroup of polyester urethanes showed a $\Delta\nu_s = 109 \text{ cm}^{-1}$, indicating that, besides the urethane C=O groups, a significant amount of hydrogen bonding also exists with ester C=O groups.

In the carbonyl stretching region of EPU09 and EPU10 (see Fig. 4), we observed a shoulder at 1700 cm^{-1} , typically assigned to hydrogen-bonded urethane carbonyls. The frequency band at 1736 cm^{-1} is assigned to the “free” carbonyls. The intermediate frequency band at 1715 cm^{-1} could be attributed to hydrogen-bonded ester carbonyls and/or irregularly hydrogen-bonded urethane carbonyls. In the carbonyl stretching region of EPU11 and EPU12 (see Fig. 5), the shoulder has become weaker and the band has become narrower and more symmetrical. Furthermore, the band of EPU12 appears to have only two main components.

There are two main possibilities of hydrogen-bond formation, i.e., ester–urethane and urethane–urethane hydrogen bonding. An attempt was made to assess the relative contribution made to the hydrogen bonding in such systems by the two potential acceptors: ester and urethane carbonyls. Seymour et al.¹⁶ concluded that essentially all the N—H groups are involved in hydrogen bonding in both polyether (PTMG) and polyester (PTMA) polyurethanes derived from MDI and BDO. It was estimated that about 60% of the N—H groups in the polyether system were associated with the hard-block urethane carbonyls (urethane–urethane hydrogen bonding), the rest being associated with the

Table III Curve-fitting Analysis Results of the C=O Stretching Region for each Polyurethane Sample

Sample	“Free” C=O			Hydrogen-bonded C=O					
	ν_f (cm^{-1})	% C=O	Width	ν_{b1} (cm^{-1})	% C=O	Width	ν_{b2} (cm^{-1})	% C=O	Width
0.9	1737	62	36.5	1715	18.9	40.1	1701	18.7	22.4
1.0	1738	60.5	36.	1714	19.5	39.	1700	17.5	23.
1.1	1738	59.7	46.2	1710	25.1	22.5	1697	13.9	22.
1.2	1737	78	36.3	—	—	—	1705	23.2	28.3

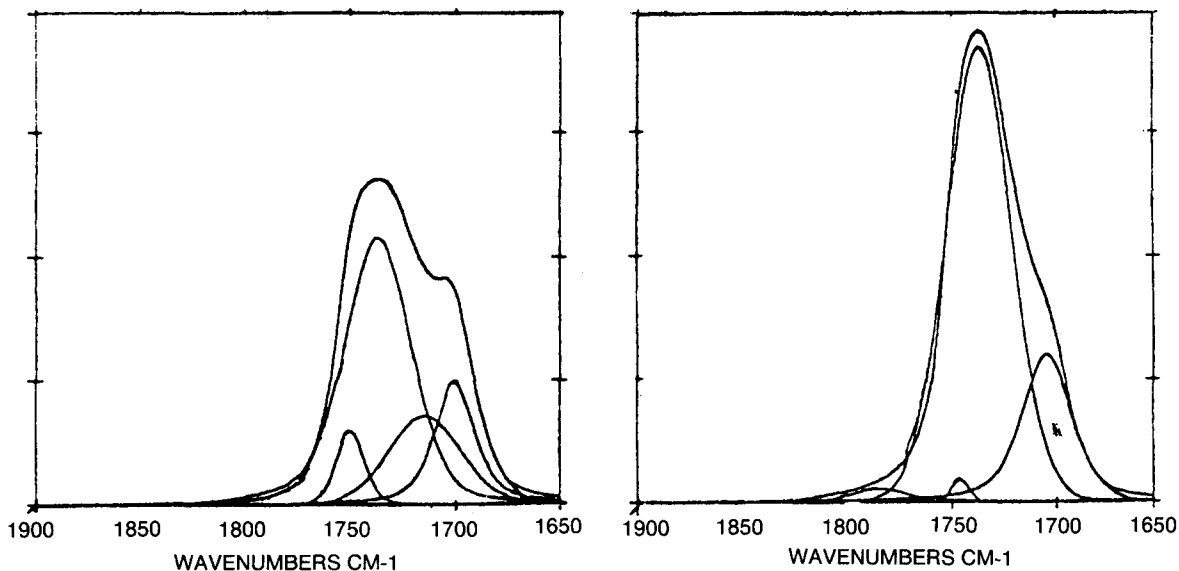


Figure 5 Curve-fitting analysis in the C=O stretching region of two representative samples with NCO/OH ratio values 0.9 and 1.2, respectively.

soft-block ether oxygens (urethane-soft block hydrogen bonding).

In the present study, the concentration of "free" carbonyl groups increases gradually as the NCO/

OH ratio increases. Therefore, for the EPU09 sample, it is estimated that roughly 62% of the total carbonyl groups are not hydrogen-bonded, whereas for the EPU12 sample, this figure has risen to 78%,

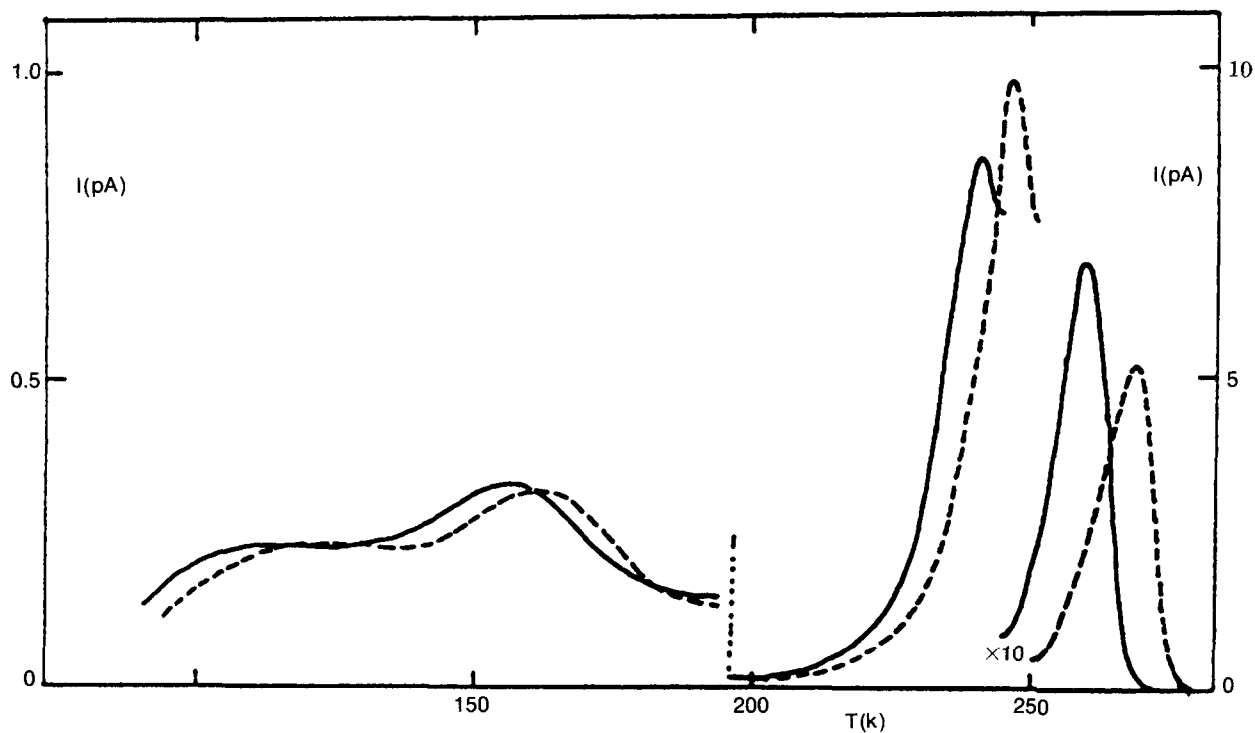


Figure 6 TSDC plots for two different types of polyurethane block copolymers, normalized to the same polarizing field of 3.5 kV/cm. Bold curve: NCO/OH = 0.9 (thermoplastic behavior). Dashed curve: NCO/OH = 1.2 (elastomeric behavior).

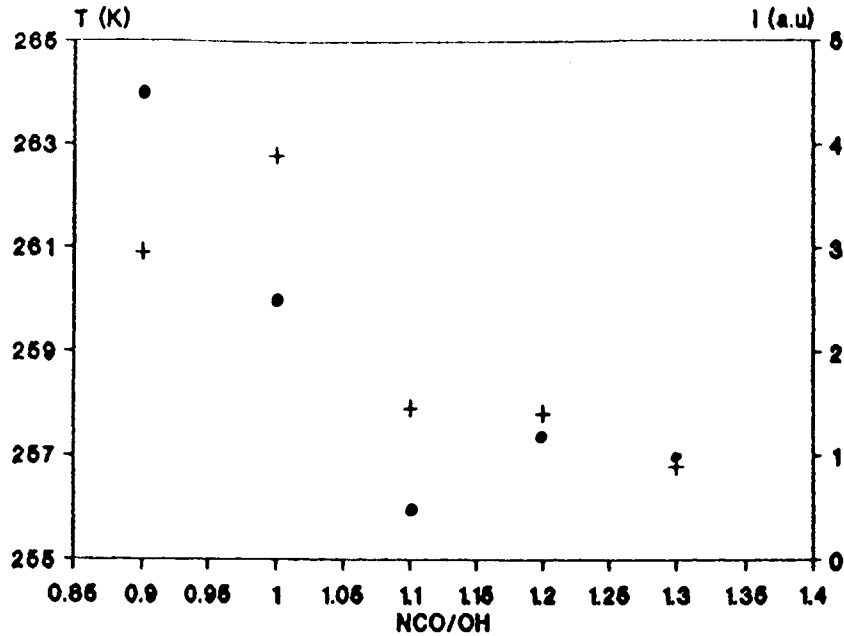


Figure 7 Variation with the NCO/OH ratio, of (■) peak temperature T_m and (+) normalized current maxima I_m of peak I.

indicating a higher degree of phase mixing. Since most of the dissolved hard segments are surrounded by the soft segments, most urethane carbonyl groups are free of hydrogen bonding. However, the results should be treated with caution since the absorption

coefficients of the three carbonyl bands making up the amide I band envelope (i.e., "free" and ordered plus disordered hydrogen-bonded) were assumed to be equal. However, as has been shown by Coleman et al.,¹⁴ the three absorptivity coefficients were not

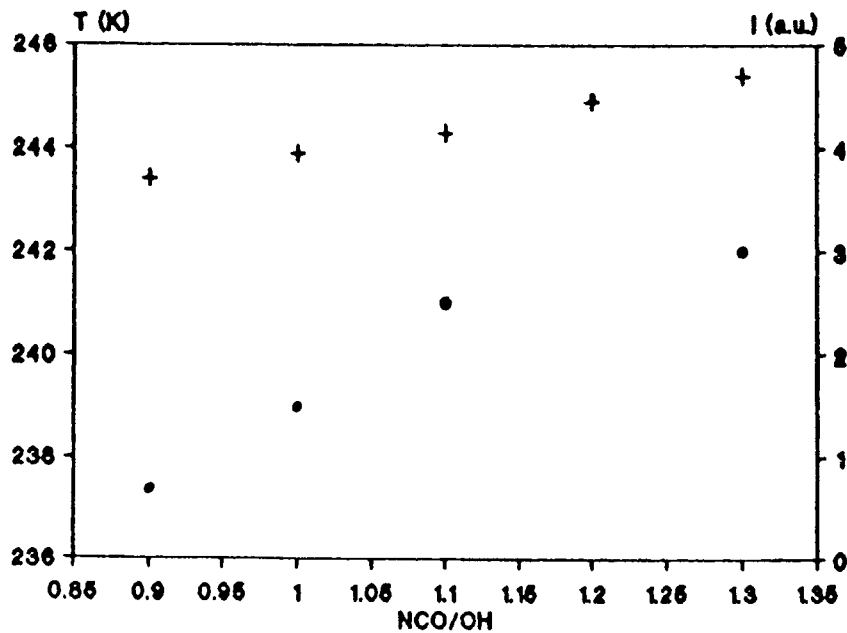


Figure 8 Variation with the NCO/OH of (■) peak temperature T_m and (+) normalized current maxima I_m of peak II.

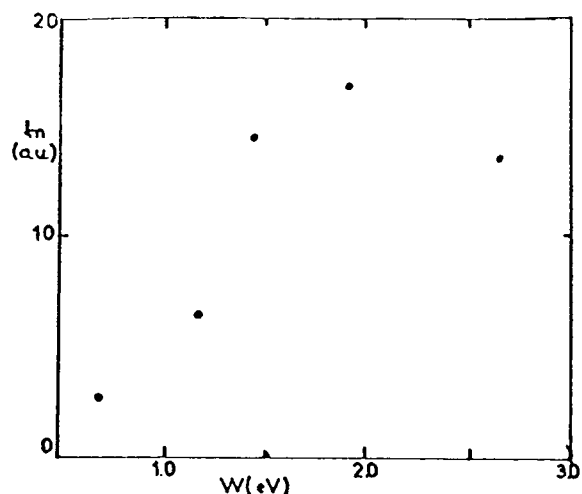


Figure 9 A typical activation energy spectrum of peak I obtained by TS analysis.

radically different. More particularly, the absorptivity coefficients of the ordered and disordered hydrogen-bonded carbonyl bands are almost equal. This is convenient for quantitative analysis.

As far as the TSDC results are concerned, the low-temperature peaks may be attributed to β and γ relaxations, respectively, observed in polyurethanes and polyamides.¹⁷ In a previous work⁷ on a series of thermoplastic polyurethanes that exhibited spectra of the same form, it was shown that the low-temperature peaks have practically the same shape,

position, and magnitude irrespectively of the hard-segment content.

In the same work, it was established that peak I is of dipolar origin, whereas peak II is due to Maxwell-Wagner-Sillars (MWS) polarization, rather than to space charges related to dc conductivity. The TS analysis of peak I showed a relaxation mechanism characterized by a continuous distribution of relaxation times with activation energy values ranging continuously from 0.70 to 2.65 eV, with a dominant value of about 2 eV (see Fig. 9). The activation energy values obtained by the TS analysis of peak I are rather high for thermally activated localized motions and justify the attribution of peak I to the glass transition of the soft part of the copolymer. As is shown in Figure 10, the high values of the activation energy (and the calculated corresponding very low values of the preexponential factor τ_0) suggest that this relaxation is related to a cooperative type of motion.

As can be seen in Figure 7, the maximum temperature of peak I shifts to higher values by increasing the NCO/OH ratio. The introduction of chemical cross-links disrupted the hard domains, increasing the possibility of intermixing of the isocyanate and ester groups. Moreover, the intermixing allows the formation of additional hydrogen bonds and this is reflected in the shift of the peak temperature. Increasing the NCO/OH ratio led to a slight increase in the intensity of peak I. A possible explanation of the observed behavior is that, since peak I is associated with motion of the dipoles in

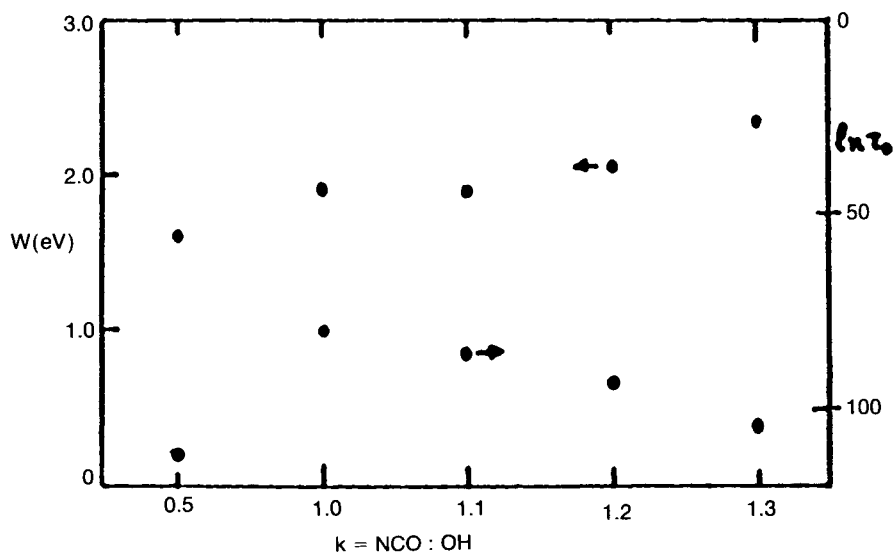


Figure 10 The activation energy and the preexponential factor of the main component of peak I obtained by TS analysis vs. the NCO/OH ratio.

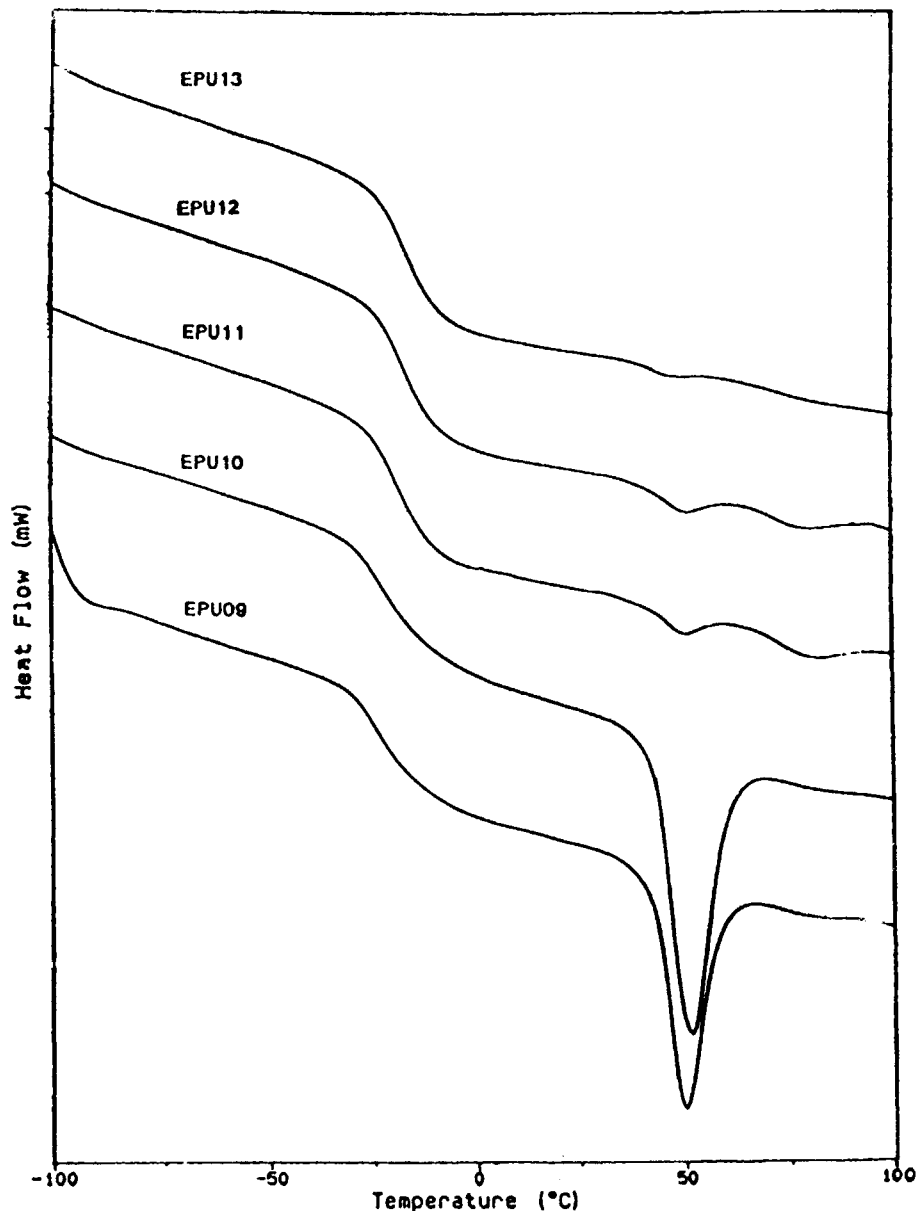


Figure 11 DSC thermograms of the five investigated samples in the -100 to $+100^{\circ}\text{C}$ temperature range.

the ethylene adipate soft part and since the prepolymer composition is constant in all samples, it is expected that the intensity of the peak is also constant. The variation of the NCO/OH ratio does not seem to affect significantly the spectrum of activation energies characterizing the glass transition relaxation (see Fig. 9). As can also be seen in Figure 10, the activation energy of the main component of peak I increases slightly by increasing the NCO/OH ratio.

As the NCO/OH ratio increases, the area of peak II diminishes significantly and the peak temperature shifts to lower values. Since peak II was attributed to interfacial MWS polarization, the decrease of the peak intensity may indicate the dismantling of the interfacial region caused by the introduction of chemical cross-links that release the space charges that have been trapped in the interface region.

The fact that the observed decrease of the magnitude of peak II by increasing the NCO/OH ratio

Table IV The Glass Transition Temperature, T_g , and the Heat Capacity Changes, ΔC_p , Accompanying This Transition

Sample	T_g ($^{\circ}\text{C}$)	ΔC_p ($\text{J/g } ^{\circ}\text{C}$)
0.9	-30.3	0.57
1.0	-29.	0.57
1.1	-26.	0.54
1.2	-24.	0.54
1.3	-23.5	0.56

is not accompanied by a corresponding significant increase in the intensity of peak I is an indication that if a dipolar contribution to molecular mobility of the interface exists in peak II this is not expected to be significant. This could possibly explain the slight increase of peak I intensity by increasing the NCO/OH ratio. The observed TSDC data do not seem to contradict the three phase model proposed by Delidis and Pethrick¹⁸ and extended by Mahboubian Jones et al.¹⁹

The DSC results show the same shifting of the glass transition temperature by increasing the NCO/OH ratio with that of peak I from the TSDC data. In addition, the heat-capacity changes, ΔC_p , accompanying this transition have essentially the same value for all the polyurethanes (see Table IV).

The endotherm at 50 $^{\circ}\text{C}$ is attributed to the melting of the crystalline soft segment. As has been reported elsewhere,²⁰ the presence and amount of soft-segment crystallinity is an indication of the extent of phase separation. On immediately rescanning, this endotherm disappears. As can be seen in Figure 11, samples with NCO/OH < 1 exhibit phase separation, whereas samples with NCO/OH > 1 have a substantial number of hard domains dissolved in the soft matrix. Incorporation of hard segments into the soft part will reduce the mobility and hamper the creation of crystalline regions.

The peak at 80 $^{\circ}\text{C}$ is associated with the disruption of disordered domains (or mixed interfacial regions). The morphology of this peak can be improved by annealing. As can be seen in Figure 11, the area of this peak diminishes and vanishes for NCO/OH > 1.2.

Summarizing the enthalpies of fusion, which are correlated to the number of hard domains, and the peak temperatures, which are correlated to the stability of the hard domains, it is observed that the ΔH_{tot} of EPU10 is larger than that of EPU09, meaning a larger number of hard domains are irregularly shaped. The ΔH_{tot} of EPU11 is smaller than that of

EPU10 and the (average) peak temperature of its main endotherm drops to lower temperatures, indicating that we have a continuous distribution of hard domains and that the percentage of hard domains has decreased. In the case of EPU12, the ΔH_{tot} is growing again and the peak temperature of the main endotherm shifts to higher temperatures. A possible explanation for this behavior considers the detrimental action of water traces that are thought to exist, even after thorough dehydration, in the commercial raw materials (polyethylene adipate and 1,4-butane diol) or in the atmosphere as moisture during pouring of the mixture onto the molding plates and the curing that followed at room temperature for 0.5 h. The reaction of water molecules with NCO groups leads to the formation of urea bonds and, consequently, to further chain extension and increasing the hard-segment length. The rest of the excess of the NCO groups was spent for the formation of biuret and allophanate cross-links.

It is observed that even the sample EPU13 exhibits a substantial amount of hard domains, although more uniformly distributed. Besides the above explanation, the introduced allophanate cross-

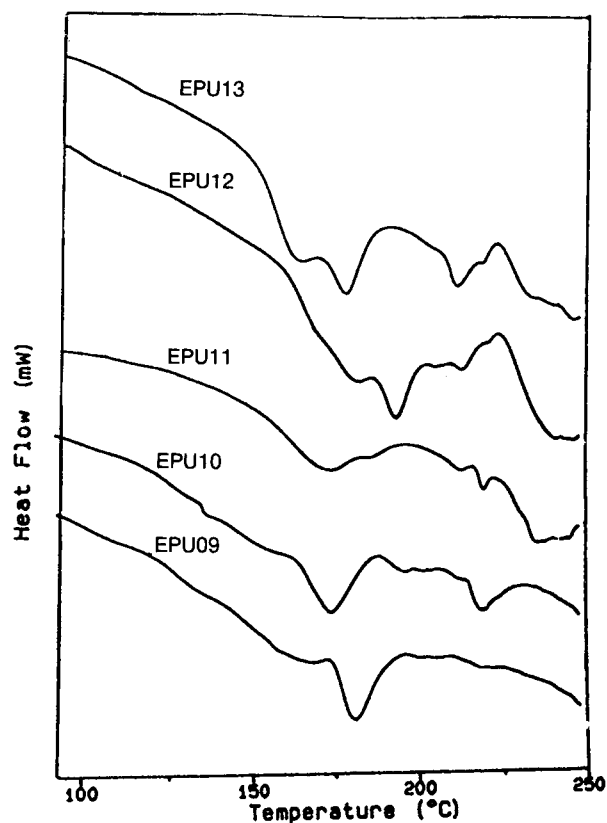


Figure 12 DSC thermograms of the five investigated samples in the 100–250 $^{\circ}\text{C}$ temperature range.

links are considered to be relatively longer than are those encountered in peroxide- or sulfur-cured polyurethanes and the result is that the network is held together less tightly.²¹ Therefore, in contrast with other polyurethane elastomers, the molecular chains are still free to align themselves and form hard domains, although of smaller size.

REFERENCES

1. R. W. Seymour and S. L. Cooper, *Macromolecules*, **6**, 48 (1973).
2. D. C. Allport and A. A. Mohajer, in *Block Copolymers*, D. C. Allport and W. H. Janes, Eds., Applied Science, London, 1973.
3. S. L. Cooper and J. C. West, *Encyclopedia of Polymer Science and Technology*, Supplement, No. 1, Wiley, New York, 1978.
4. R. P. Redman, in *Developments in Polyurethanes*, J. M. Buist, Ed., Applied Science Publishers, London, 1978, Chap. 3.
5. A. Noshay and J. E. McGrath, *Block Copolymer—An Overview and Critical Survey*, Academic Press, New York, 1978, p. 389.
6. W. Nierzwicki and J. Wysocka, *J. Appl. Polym. Sci.*, **25**, 739–746 (1980).
7. E. Kontou, G. Spathis, M. Niaounakis, and V. Kefalas, *Colloid Polym. Sci.*, **268**, 636–644 (1990).
8. H. S. Lee, Y. K. Wang, and S. L. Hsu, *Macromolecules*, **20**, 2089 (1987).
9. H. S. Lee, Y. K. Wang, W. J. MacKnight, and S. L. Hsu, *Macromolecules*, **21**, 270 (1988).
10. Y. Camberlin and J. P. Pascault, *J. Polym. Sci. Polym. Phys. Ed.*, **22**, 1835 (1984).
11. R. Zielinski and M. Rutkowska, *J. Appl. Polym. Sci.*, **31**, 1111–1118 (1986).
12. J. Vanderschueren and J. Gasiot, in *Thermally Stimulated Relaxation in Solids*, P. Braunlich, Ed., Springer, Berlin, 1979, pp. 135–223.
13. C. M. Brunette, S. L. Hsu, and W. J. MacKnight, *Macromolecules*, **15**, 71–77 (1982).
14. M. M. Coleman, K. H. Lee, D. J. Skrovanek, and P. C. Painter, *Macromolecules*, **19**, 2149–2157 (1986).
15. Yu. M., Boyartchuk, L. Ya. Rappoport, V. N. Nikitin, and M. Apukhtine, *Polym. Sci. USSR*, **7**, 859 (1965).
16. R. W. Seymour, G. M. Esters, and S. L. Cooper, *Macromolecules*, **3**, 579 (1970).
17. P. Hedvig, *Dielectric Spectroscopy of Polymers*, Hilger, Bristol, 1977.
18. C. Delidis and R. A. Pethrick, *Eur. Polym. J.*, **17**, 675–681 (1981).
19. M. G. B. Mahboubian Jones, D. Hayward, and R. A. Pethrick, *Eur. Polym. J.*, **23**(11), 855–860 (1987).
20. C. A. Burne, D. P. Mack, and J. M. Sloan, *Rubber Chem. Technol.* **58**(5), 985–996 (1985).
21. P. Wright and A. P. C. Cumming, *Solid Polyurethane Elastomers*, Maclaren and Sons, London, 1969, Vol. 10, pp. 207–208.

Received July 7, 1993

Accepted February 28, 1994